Available online at www.sciencedirect.com
SCIENCE DIRECT®
Catalysis Today 98 (2004) 375–385
CATALYSIS TODAY
www.elsevier.com/locate/cattod

Development and optimization of NO_x storage and reduction catalysts using statistically guided high-throughput experimentation

Reed J. Hendershot[a], W. Benjamin Rogers[a], Christopher M. Snively[a,b], Babatunde A. Ogunnaike[a], Jochen Lauterbach[a,*]

[a]*Department of Chemical Engineering, University of Delaware, Newark, DE 19716, USA*
[b]*Department of Materials Science and Engineering, University of Delaware, Newark, DE 19716, USA*

Available online 27 September 2004

Abstract

The interaction between reaction conditions and catalyst compositions for NO_x storage and reduction (NSR) catalysts has been explored using a combination of high-throughput experimentation and experimental design. This was accomplished by varying the concentration of NO and O_2, the reducing agent concentration and identity, space velocity, and reactor temperature. All reaction conditions were varied simultaneously for a range of Pt, Ba, and Fe loadings on γ-Al_2O_3. It was found that most of the reaction conditions investigated affected the saturation NO_x storage, the production of nitrous oxide, and the steady state lean NO_x reduction. An empirical model was developed using response surface methodology to predict the saturation NO_x storage and nitrous oxide production as a function of Pt, Ba, and Fe weight loading. This model was used to optimize the catalytic composition and a comparison between the model predictions and experimental results for the optimized catalysts are given. It was shown that high-throughput experimentation in combination with experimental design leads to more efficient use of experimental resources in addition to a more in depth understanding of catalytic systems.

Keywords: NO_x storage and reduction; Sulfur poisoning; High-throughput experimentation; Heterogeneous catalysts; Design of experiments; Screening design; Factorial design; Response surface design

1. Introduction

Lean burn gasoline engines have been promoted as a method to improve the fuel efficiency of automobile engines, decrease dependence on non-renewable petroleum, and reduce the emission of greenhouse gases. Impeding the widespread implementation of lean burn engines is the inability of current three-way catalytic converters (TWC) to reduce nitrogen oxides (NO_x) under net-oxidizing conditions. Extensive research has been performed in search of alternative catalysts that will reduce NO_x in oxygen rich environments under steady state conditions, but an acceptable catalyst has not yet been discovered [1–3].

To address the apparent conflict of high efficiency and low NO_x emissions, NO_x storage and reduction (NSR) catalysts were designed to store NO_x during a fuel lean cycle and reduce the stored NO_x during a subsequent fuel rich cycle [4–8]. Extensive research has been performed on NSR catalysts in the past decade to understand the storage and reduction mechanisms and improve overall NO_x conversion [9–24]. Since NSR catalysts are very susceptible to sulfur poisoning, several studies have also examined the effect of sulfur on NSR catalysts [25–34]. In spite of the extensive literature, there have not been reports demonstrating NSR catalytic performance over a wide range of operating conditions for catalysts of varying compositions.

Reaction conditions affecting NSR catalysts include temperature, NO_x concentration, O_2 concentration, CO_2 concentration, reductant concentration, reductant type, space velocity, total lean/rich cycle time, lean/rich duty cycle, and the presence of sulfur and water. In addition to reaction conditions, the performance of NSR catalysts is strongly influenced by the catalyst composition. Therefore, describing NSR catalytic performance requires not only understanding the effect of the reaction conditions on a

* Corresponding author. Tel.: +1 302 831 6327; fax: +1 302 831 1048.
E-mail address: lauterba@che.udel.edu (J. Lauterbach).

0920-5861/$ – see front matter © 2004 Elsevier B.V. All rights reserved.
doi:10.1016/j.cattod.2004.08.005

single catalyst, but also how these effects change as the composition of the catalyst changes.

To study such a complex system in a systematic manner with conventional methodologies would require an extensive experimental effort. Just considering 10 different catalysts, studied over five different reaction condition parameters, each varied over five levels, would lead to 31,250 different experiments (10×5^5). Assuming that one catalyst could be tested at 10 different conditions in a single day and that no repeat runs were performed, it would take over 3000 working days to complete the experimental effort. To increase the throughput at which catalytic systems can be studied, high-throughput experimentation (HTE) approaches are increasingly used for materials development [35,36]. High-throughput catalytic techniques have been used to study selective catalytic reduction of nitric oxide using hydrocarbons [37–40] and one study looked at seven catalysts for NO_x storage activity under a single reaction condition [40], but to the best of our knowledge, there have been no published reports using HTE to study NSR catalysts under transient conditions over a large parameter space.

Even with HTE, it is experimentally expensive to study the entire range of combinations and concentrations affecting NSR catalysts in a reasonable amount of time. Therefore, we are employing a combination of statistical design of experiments (DOE) [41] and HTE to study NSR catalysts over a wide range of reaction conditions and catalyst compositions. Statistical experimental design methods have been applied to zeolite synthesis [42], catalyst optimization and discovery for a single reaction condition using HTE [43,44], reaction condition optimization for single catalysts discovered with HTE [45], and recently discussed in the literature, without the use of experimental data, as a tool in HTE [46]. A recent paper presents the application of DOE to HTE in studying both the catalyst composition and the reaction conditions [47]. This paper, however, does not provide enough details about the procedure used to generate the design and it is uncertain to what extent interactions were studied and how the optimization was conducted. In the results presented below, we will provide details of the experimental procedure and demonstrate the application of HTE to the study of NSR catalysts in combination with experimental design.

2. Experimental

2.1. High-throughput experimental setup

Our group has developed a quantitative, high-throughput analytical technique based on Fourier transform infrared (FT-IR) imaging [48–52] that is capable of studying 16 samples simultaneously under realistic reaction conditions. The setup consists of a Bruker Equinox 55 FT-IR spectrometer interfaced with a 64×64 pixel mercury cadmium telluride FPA detector (Santa Barbara Focalplane, Goleta, CA, USA), and is capable of collecting IR spectra of the effluents of all 16 reactors in less than 2 s. Details of the optical setup and analytical methods can be found in [48,52]. The system produces data of comparable quality to that obtained from single reactor studies [53], and is capable of studying both steady state and transient reaction kinetics in parallel [54]. Briefly, the reactors are vertical flow-through reactors with a catalyst powder supported on a stainless steel frit. Each reactor contains a thermocouple in the catalyst bed, and the temperatures of all 16 reactors are continuously displayed and recorded by software written in house using LabView®. Multiple mass flow controllers permit a wide range of feed gas concentrations, compositions, and flowrates to be explored. In addition, an orifice and a needle valve are installed before each reactor to minimize any flowrate differences among the different reactors. The flowrates were measured and recorded using a digital flowmeter (Agilent—ADM 2000) and a computer controlled switching valve.

2.2. Statistical experimental design

The basic premise of all experimental research is that experimental data contain information from which understanding can be extracted. However, *if the data are not acquired carefully, one may end up with data that do not contain the required information*. Additionally, *any information not contained in data cannot be extracted even by the most sophisticated analysis*. Ensuring that one is able to acquire informative data in the face of unavoidable random variability, and extract the contained information efficiently, is the role of statistical design of experiments. For high-throughput studies, where one is able to acquire large quantities of data in short periods of time, the judicious application of experimental design is especially important.

Statistical experimental design procedures have been used successfully in many science and engineering applications [55,56]. The fundamental goal of these procedures is adequacy and efficiency. Adequacy is ensuring that the acquired data contain the information required to achieve the objectives of the experimental study, and efficiency is obtaining the desired information with the minimum number of experiments. Given the possibility of different objectives at different phases of experimental studies, there are various experimental designs for each phase. In this paper, we will discuss the application of screening designs and response surface designs, using HTE, for the development of NSR catalysts.

For this study, fractional and full factorial designs were used as screening designs. At this level of experimentation, a linear model was developed relating a performance criterion (Y) to the parameters of interest ($X_1, X_2, X_3, \ldots$). This model takes the form of

$$Y = C + \alpha_1 X_1 + \alpha_2 X_2 + \alpha_3 X_3 + \cdots + \alpha_{12} X_1 X_2 + \alpha_{13} X_1 X_3 + \cdots + \alpha_{123} X_1 X_2 X_3 + \cdots \quad (1)$$

where C is a constant and α_i are coefficients fitted to the experimental data. This level of experimentation allowed the determination of important parameters and the interactions between them. To decrease the number of experiments required in a screening design, a fractional factorial design was used, in which a fraction of the full factorial design was performed. This resulted in a significant decrease in the experimental effort by combining the effects of higher order interactions with lower order interactions.

Once the important parameters were identified, a response surface study was completed to refine the model and optimize the catalyst and reaction conditions. The response surface model takes the form of

$$Y = C + \alpha_1 X_1 + \alpha_2 X_2 + \cdots + \alpha_{12} X_1 X_2 + \cdots + \beta_1 X_1^2 + \beta_2 X_2^2 + \cdots \quad (2)$$

where β_i are the coefficients for the squared terms in the model. Three-way (i.e. $X_1X_2X_3$) and higher interactions were excluded.

2.3. Catalyst preparation and performance analysis

The NSR catalysts were synthesized with Pt, Ba, and Fe supported on γ-Al_2O_3 (Catalox® Sba-200, 200 m^2/g). Pt and Ba were chosen as typical NSR components, and Fe was added because of reports that it improved the resistance of Pt/Ba NSR catalysts to sulfur [57]. All catalysts were synthesized utilizing incipient wetness. Chloroplatinic acid hexahydrate, barium nitrate, and iron (III) nitrate nonahydrate precursors (Strem Chemicals) were dissolved in distilled water before impregnation. Because of the low solubility of $Ba(NO_3)_2$ in water, it was necessary to utilize multiple impregnation steps to achieve the desired weight loadings. This was accomplished by dissolving the necessary amount of all precursors in distilled water to obtain the weight loading for a given catalyst. This solution was added to the dried support until incipient wetness was obtained. The impregnated supports were dried overnight in a vacuum oven at a temperature of ∼393 K and then crushed before the next impregnation step. This process was repeated until the entire precursor solution had been added to the support.

After completion of the final impregnation step, the powders were crushed and calcined in a tube furnace. The calcination procedure consisted of heating to 473 K over 2 h, holding the temperature at 473 K for 1 h, further heating to 823 K over 3 h, holding at 823 K for 2 h, and then cooling to 298 K over 4 h. Before the first run, the catalysts were reduced in the high-throughput reactor for 1 h in 10% v/v H_2 at 773 K. On subsequent days, the catalysts were reduced for 30 min under identical conditions. The naming convention for each catalyst is based on the nominal weight loading. Thus, a catalyst with a nominal weight loading of 1% w/w Pt and 15% w/w Ba is referred to as 1Pt/15Ba. For all results reported, 0.15 g of catalyst was loaded into each reactor.

The gases used in the experiments were obtained from BOC Gases and Keen Compressed Gas. The nitric oxide (NO) and sulfur dioxide (SO_2) were obtained as premixed 1% NO in He and 5000 ppm SO_2 in He. Ethylene, carbon monoxide, oxygen, hydrogen, and helium, were obtained at purity levels ≥99.99%.

The catalysts were studied with respect to three performance criteria: saturation NO_x storage (SNS) capacity, total nitrous oxide (N_2O) production (NOP), and the steady state lean NO_x reduction (LNR) to both partially reduced nitrous oxide and fully reduced molecular nitrogen (N_2).

The three different performance criteria are defined in Fig. 1, along with typical data acquired during a switch from fuel rich to fuel lean conditions. Fuel rich and fuel lean conditions refer to the molar ratio of oxidizing to reducing molecules as defined by the stoichiometric ratio (SR):

$$\mathrm{SR} = \frac{[\mathrm{NO}] + 2[\mathrm{O_2}]}{[\mathrm{CO}] + 6[\mathrm{C_2H_4}]} \quad (3)$$

SR greater than 1 refers to fuel lean conditions, while SR less than 1 refers to fuel rich conditions. To convert from fuel rich to fuel lean experimentally, a portion of the helium in the reactant gases was replaced with an equal volume of O_2 using a four-way switching valve. The pressures of the switching valve outlets were balanced to maintain a constant flowrate and pressure to the reactor inlets while changing the reactant concentrations.

SNS is defined as the area between the steady state NO_x concentration in the fuel lean state and the actual effluent concentration of NO_x from the time at which O_2 was added to the feed gases. NOP is defined as the total production of N_2O after the switch from fuel rich to fuel lean. Since the flowrates were recorded for each reactor, the integrated areas for SNS and NOP were converted to moles of NO_x and N_2O, respectively. LNR activity is defined as the percentage difference between the inlet NO concentration and the steady state NO_x concentration in the fuel lean state.

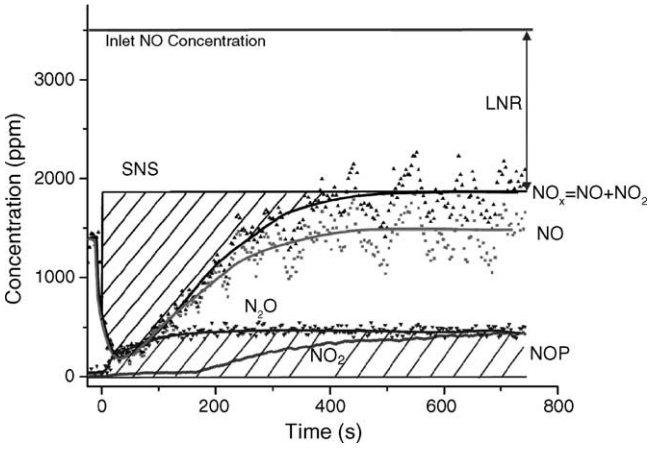

Fig. 1. Typical data collected during a switch in the reaction conditions from fuel rich to fuel lean showing saturation NO_x storage, N_2O production, and lean NO_x reduction.

A difficulty arises in analyzing the high-throughput transient data. The only change between the fuel rich state and the fuel lean state is the replacement of a portion of the He with O_2. Since oxygen is not detected in the IR and no tracer element was included with the O_2, a method was needed used to correlate the transient IR data to the change in the reaction gases. To determine the data point at which the inlet concentration switched between fuel rich and fuel lean, one reactor tube was left empty and was used as a reference. Using this blank reactor, it was possible to determine when the gases were switched between fuel rich and fuel lean by tracking the concentration of NO_2. Upon the addition of O_2 during a switch from fuel rich to fuel lean, a portion of the inlet NO converts to NO_2. The time corresponding to the data point immediately before any detectable change in the concentration of NO_2 was defined as time for the reactant switch (t_{rs}) in the blank reactor. Despite the best of efforts, the flowrates for all reactors were not exactly equal, and it was therefore necessary to relate t_{rs} in the blank reactor to t_{rs} in the other reactors. This was done by converting the increment between infrared spectra, and therefore data points collected at a constant rate of one every 3.07 s, to inlet moles of NO_x using Eq. (4)

$$\text{Inlet } NO_x = \frac{t_s W P X_{NO}}{RT} \quad (4)$$

where R is the universal gas constant, t_s the time in seconds elapsed from when the first spectrum was collected, W the volumetric flowrate for each reactor, P the pressure, X_{NO} the inlet NO mole fraction, and T the temperature. Once the data for all reactors were referenced to inlet moles of NO_x, the total number of inlet moles of NO_x corresponding to t_{rs} in the blank reactor was assumed to be equal for the remaining 15 reactors and t_{rs} for all reactors was then determined.

3. Screening design

3.1. Experiments without SO_2

For the screening design, we studied the significance of the weight loadings of Pt, Ba, and Fe as well as catalyst temperature, NO_x concentration, O_2 concentration, reductant concentration, reductant type, and space velocity. The high and low settings for the metal loadings were 0 and 1% w/w Pt, 0 and 15% w/w Ba, and 0 and 5% w/w Fe, respectively. The nominal compositions of the synthesized catalysts are summarized in Fig. 2, where the position of each circle indicates the nominal weight loading. In the screening design, a full factorial design was used for the catalytic composition, resulting in a total of eight catalysts (shown as white circles in Fig. 2). Since the reactor is capable of testing 16 catalysts simultaneously, each sample was placed into two reactors to test for reproducibility between reactors. The support material alone was placed into one reactor, and the remaining reactor was left without any catalyst to be used as the reference reactor (referred to as ''blank'' in the figures and tables).

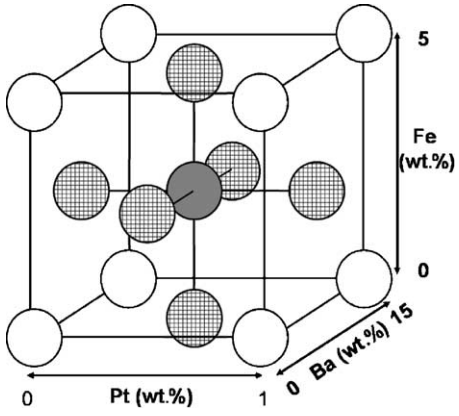

Fig. 2. Nominal weight loadings of the synthesized catalysts are indicated by the location in this diagram of a three-dimensional box. The unfilled circles indicate catalysts studied in the screening design. The cross filled and solid filled circles indicate the additional catalysts studied in the response surface design.

The high and low settings for the fuel lean inlet reaction conditions used as input to the fractional factorial design are shown in Table 1. In this design, either ethylene or carbon monoxide was used as the reducing agent. The concentration of the two reducing agents was chosen to assure that the stoichiometric ratio between the oxidizing and reducing agents remained constant. A quarter fraction factorial design was used to reduce the number of experimental conditions from 2^6 (64) to 2^{6-2} (16). The actual reaction conditions tested are listed in Table 2. All screening catalysts were tested at all screening design reaction conditions listed.

Before collecting data, at least two lean/rich cycles of 14 min lean and 6 min rich were completed for the given reaction condition. These cycle times were chosen so the effluent from all reactors reached steady state. After the initial lean/rich cycles were completed, IR spectra were

Table 1
Reaction condition screening parameters investigated

Setting	NO concentration (ppm)	O_2 concentration (%)	CO concentration (%)	C_2H_4 concentration (%)	Reductant type	Space velocity (mL/h/g_{cat})	Temperature (K)	SO_2 concentration (ppm)
Low	3500	4	3.5	0.58	C_2H_4	30000	548	0
High	8650	8	5.5	0.92	CO	42500	648	300

Table 2
Actual reaction conditions tested on all screening catalysts

Reaction condition (ID)	NO concentration (ppm)	O_2 concentration (%)	CO concentration (%)	C_2H_4 concentration (%)	Space velocity (mL/h/g_{cat})	Temperature (K)	Stoichiometric ratio	
							Lean	Rich
1	3500	8		0.92	30000	548	2.97	0.06
2	8650	4	5.5		30000	548	1.61	0.16
3	3500	4	5.5		42500	548	1.52	0.06
4	3500	8	3.5		42500	548	4.67	0.10
5	8650	8		0.92	42500	548	3.07	0.16
6	3500	4		0.58	30000	548	2.39	0.10
7	8650	8	3.5		30000	548	4.82	0.25
8	8650	4		0.58	42500	548	2.53	0.25
9	8650	8		0.58	30000	648	4.82	0.25
10	8650	4	3.5		42500	648	2.53	0.25
11	3500	8		0.58	42500	648	4.67	0.10
12	3500	4	3.5		30000	648	2.39	0.10
13	8650	4		0.92	30000	648	1.61	0.16
14	3500	8	5.5		30000	648	2.97	0.06
15	3500	4		0.92	42500	648	1.52	0.06
16	8650	8	5.5		42500	648	3.07	0.16

collected continuously during the switch from fuel rich to fuel lean and then back again to fuel rich. The collection time in the fuel lean and fuel rich phases was maintained at 14 and 6 min, respectively.

3.1.1. Results and discussion—saturation NO_x storage

All catalysts were first tested for SNS for the reaction conditions listed with CO as the reducing agent (referred to as Group 1 and listed as runs 2–4, 7, 10, 12, 14, and 16 in Table 2, respectively). After the initial study, all conditions listed in Table 2 were then tested (referred to as Group 2). The results for the SNS as a function of reaction condition and testing group are shown in Fig. 3 for the 1Pt/15Ba/5Fe catalyst. From this figure, there appears to be a "start up" time for this catalyst in terms of its ability to store NO_x. For example, comparing reaction conditions 2, 4, 10, 12, and 14, there was an improvement between Group 1 and Group 2. However, reaction conditions 7 and 16 were very similar for the two different collections. This could indicate that the difference in catalytic performance was due to different initial conditions, i.e. a different history of reaction conditions exposed to the catalyst, and not a "start up" time.

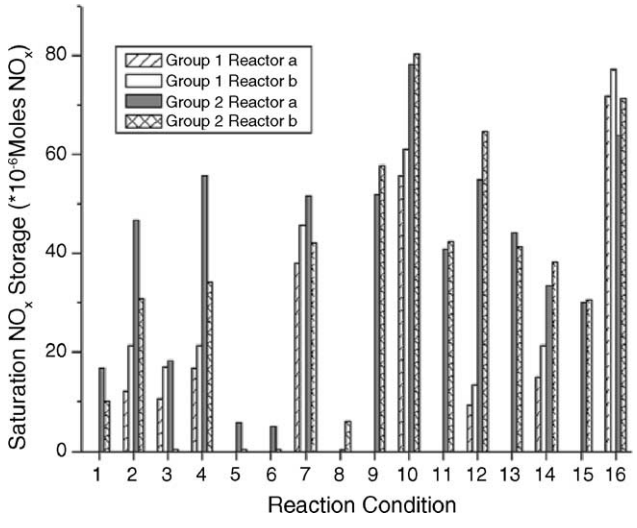

Fig. 3. Results for the saturation NO_x storage of the 1Pt/15Ba/5Fe catalyst for all reaction conditions in the screening design. The catalysts were loaded into two different reactors and tested over various days.

The difference between reactor to reactor results is normally less than 10 μmol NO_x storage (except for reaction conditions 2 and 4), as seen in Fig. 3. Comparing the SNS as a function of the reaction conditions, it can be seen that using CO as the reducing agent results in a larger SNS than ethylene (notice that reaction conditions 10, 12, and 16 all use CO as the reducing agent). Likewise, SNS at 648 K is higher than SNS at 548 K, as is already known [18,54,58]. Further quantitative analysis of the data requires the application of statistical methods to separate the effects of the six factors and their interactions from the inherent noise in the data.

Using the data set from Group 2, reactors a and b, the results shown in Table 3 for the 1Pt/15Ba/5Fe catalyst were obtained. Similar results were obtained for all catalysts studied. Table 3 includes the estimated parameters for a linear model, similar to Eq. (1), of how SNS, NOP, and LNR are affected by the reaction conditions. It should be noted that the effect of the reductant concentration is for either the C_2H_4 or the CO concentration. Only parameters significant to 95% confidence are shown. The normalized parameters and their coefficients are listed in Table 3. The normalization was accomplished by assigning the low value listed in Table 1 as −1 and the high value as +1, using Eq. (5)

$$Y(X) = \frac{2X - X_H - X_L}{X_H - X_L} \quad (5)$$

where Y is the normalized variable and X_L and X_H the low and high values, respectively, as listed in Table 1. Therefore,

Table 3
The statistical analysis of the Group 2 data for the 1Pt/15Ba/5Fe catalyst in the screening study

Normalized variables	SNS ($\times 10^{-6}$ mol NO_x) coefficient	NOP ($\times 10^{-6}$ mol N_2O) coefficient	LNR (%) coefficient
Constant	35.2	29.9	27.5
95% confidence interval (±)	2.8	1.9	1.5
Parameters			
NO	5.9	7.4	−4.9
O_2	–	−4.0	−5.8
Reductant concentration	−5.9	5.4	8
Reductant type (from C_2H_4 to CO)	12.2	−7.9	−16.4
Space velocity	–	2.7	−2.2
Temperature	16.3	−11.7	−10.8
Parameter interactions			
NO × reductant concentration	–	3.5	–
NO × reductant type	4.7	–	4.5
Reductant type × temperature	−3.1	4.9	2.9
NO × temperature	3.6	−3.3	2.1
Reductant type × reductant concentration	−4.4	–	–
NO × reductant concentration × temperature	–	−2.3	–
NO × reductant type × red concentration	3.5	–	−2.9

increasing the inlet NO concentration from 3500 to 8650 ppm, while holding everything else constant, increases the SNS by 11.8 ± 2.8 μmol NO_x, on average. The same trend holds for the remaining parameters.

The positive correlation between SNS and inlet NO concentration was caused by the accompanying increase in the NO_x gas and/or catalyst surface concentration near the Ba storage sites. This increase in NO_x concentration shifted the Ba equilibrium phase to a higher ratio of $Ba(NO_3)_2$ to $BaCO_3$ [20,59]. Although Mahzoul et al. [18] did not observe a change in SNS while changing NO concentrations, the inlet NO concentrations were significantly lower (200–1000 ppm NO) than those presently studied, and the change in NO concentration might not have been sufficient to cause a noticeable change in SNS. The results in Table 3 also indicate that the O_2 concentration is not significant between 4% v/v and 8% v/v, confirming previous studies that show the O_2 concentration only affects the SNS below 3% [18] or 4% [58].

In contradiction to the conclusions drawn by Fridell et al. [58] (who did not measure NO_x storage until steady state), our results indicate that the reductant concentration and the reductant type have an influence on the SNS. The data in Fridell et al. showed a minimal decrease in NO_x storage with increasing propylene concentration. However, since only four data points and no statistical analysis or confidence intervals were reported, it is not possible to state with certainty whether the propylene concentration affected the NO_x storage. Our results demonstrate that increasing the reducing agent concentration does decrease the SNS. Our results also indicate that SNS changes with the reducing agent, confirming results reported in [16], which show a difference between H_2 and CO, but contradicting results in [58], which showed minimal changes in NO_x storage for different reducing agents (i.e. C_3H_6, C_3H_8, CO, and H_2). It would be surprising if the reducing agent did not affect the SNS, since it is known that the reducing agent strongly affects NO reduction under lean conditions over noble metal catalysts [1,60,61]. It has also been shown that the reducing agent affects the thermal stability of NO_x species stored on Ba containing catalysts [62,63]. These effects can be explained by considering the thermodynamic driving force for the formation of $Ba(NO_3)_2$. Increasing the reductant concentration and changing the reductant type, from CO to C_2H_4, leads to an increase in LNR as seen in Table 3. Higher LNR lowers the NO_x gas and/or catalyst surface concentration near Ba storage sites. This in turn shifts the Ba equilibrium phase to a lower ratio of $Ba(NO_3)_2$ as compared to $BaCO_3$ and $Ba(OH)_2$ [20].

The results discussed in the preceding paragraphs could have been obtained from traditional methods of changing one variable at a time; however, a significantly larger number of experiments would have been required. Additionally, the interaction information shown in Table 3 could only have been obtained by varying more than one variable at a time. The results for the 1Pt/15Ba/5Fe catalyst and the other screening catalysts indicate that interactions in reaction conditions are statistically significant. Previous reports have mostly neglected the possibility of interactions. This study demonstrates the importance of a systematic analysis in the study of catalytic systems to understand not only the effects of experimental parameters in isolation, but to also understand the significance of the interactions between parameters.

Since a fractional factorial design was employed in this screening study, the interactions are combined with each other, and the most likely interactions are listed in Table 3. The results for the screening design must be understood in the context of this ambiguity. Since the interactions are uncertain at this stage of testing, they will not be discussed in more detail in this paper. In a forthcoming publication, the

significance of the interactions will be examined using the response surface approach described in Section 4.

3.1.2. Results—nitrous oxide production

Previous work by our group has shown that N_2O was produced during the switch from fuel rich to fuel lean for some NSR catalysts and reaction conditions [54]. Understanding the production of N_2O, in order to limit its production, is important for the development of NSR catalysts because of nitrous oxide's strength as a greenhouse gas and polluter [64].

Table 3 shows that the NOP depends most strongly on the temperature, inlet NO concentration, reductant concentration, and reductant type for the 1Pt/15Ba/5Fe catalyst. The NOP statistical analysis does not take into account the fact that the shape of the N_2O concentration profile during a switch from fuel rich to fuel lean depended strongly on the reductant type and catalyst. This can be seen in Figs. 4 and 5, where the transient in the N_2O production is shown for reaction conditions 4 and 8, respectively, for both the 1Pt/15Ba/5Fe and the 1Pt catalyst. In Fig. 4 CO was used as the reducing agent and there was only a transient in the N_2O production for the 1Pt/15Ba/5Fe catalyst, observed as a sharp rise followed by decay to a steady state value. This general shape is representative for all reaction conditions with CO as the reducing agent. The 1Pt catalyst does not exhibit the same behavior until the temperature is increased to 648 K (not shown). Fig. 5 also demonstrates a sharp increase in the N_2O concentration; however, the decay ends prematurely as the rate of a second reaction mechanism producing N_2O increases towards a steady state value.

These results imply that the reaction mechanism that produced the first spike in N_2O concentration is independent of the reducing agent. The temporary increase in N_2O concentration also indicates that there is a pool of N_2O precursor on the Pt catalyst surface that is converted

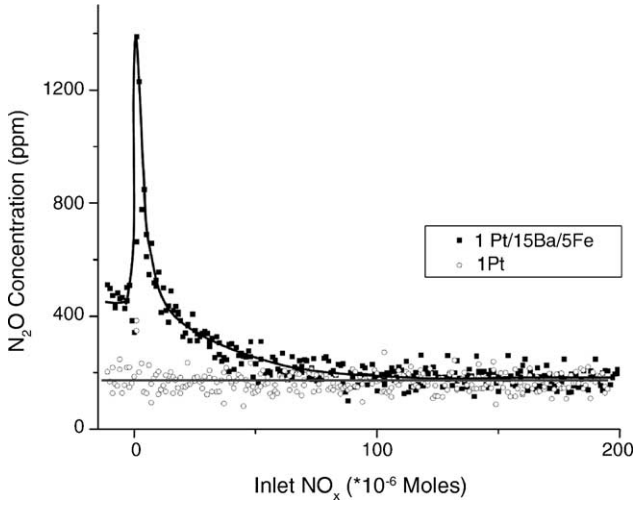

Fig. 4. The N_2O production for the 1Pt/15Ba/5Fe and 1Pt catalysts during a switch from fuel rich to fuel lean conditions under reaction condition 4.

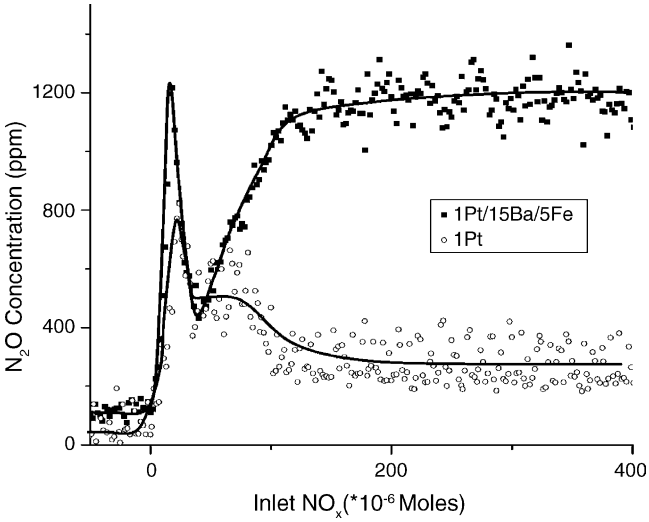

Fig. 5. The N_2O production for the 1Pt/15Ba/5Fe and 1Pt catalysts during a switch from fuel rich to fuel lean conditions under reaction condition 8.

to N_2O upon the addition of O_2. The identity of this N_2O precursor produced from NO molecules on Pt is a subject of debate in the open literature [65,66], and will not be addressed further here. Our result that the 1Pt/15Ba/5Fe catalyst demonstrated a sharp spike in N_2O production, at a temperature lower than the 1Pt catalyst, is consistent with other results showing that Ba promoted the activity of Pt in a simulated exhaust [67]. The second rate that leads to the steady state N_2O production was strongly dependent on the reducing agent in our studies, and similar results are well documented in the literature [1,60,61]. All catalysts containing Pt demonstrated results similar to the 1Pt and 1Pt/15Ba/5Fe catalysts.

3.1.3. Results—lean NO_x reduction

Extensive work has been performed on selective catalytic reduction using ammonia and hydrocarbons on both zeolitic and non-zeolitic materials [1,2]. The LNR results for the 1Pt/15Ba/5Fe catalyst are shown in Fig. 6. Here, it can be seen that at 548 K (reaction conditions 1–8) using ethylene as the reducing agent (reaction conditions 1, 5, 6, 8, 9, 11, 13, and 15) resulted in higher LNR compared to CO as the reducing agent. The reaction conditions that resulted in the highest SNS (i.e. 9, 10, 12, and 16) resulted in some of the lowest LNR activities. The negative correlation between SNS and LNR was discussed in Section 3.1.1. These qualitative observations are confirmed by the analysis in Table 3 where the strongest factors affecting LNR are reductant type and temperature. The effect of temperature is not surprising, as it has been previously demonstrated that selective catalytic reduction depends strongly on temperature [1]. A dependence of LNR on reducing agent has also been reported [62,63].

The effect of the NO, O_2, and reducing agent concentration can be explained by their effect upon the stoichiometric ratio. Increasing both NO and O_2 concentrations

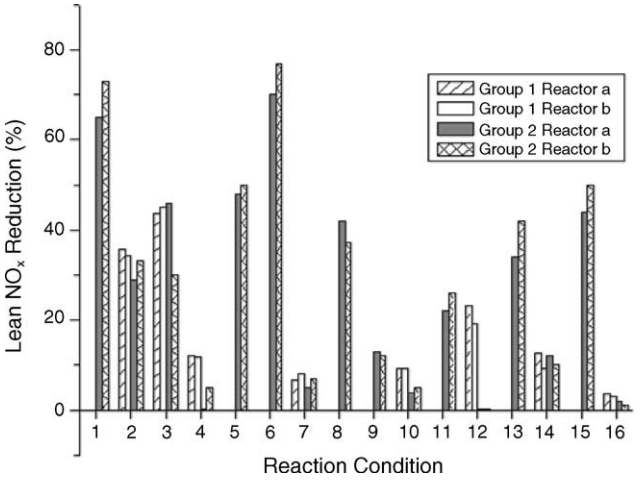

Fig. 6. The lean NO_x reduction for the 1Pt/15Ba/5Fe catalyst as a function of reaction condition during the screening design.

increases the stoichiometric ratio and causes the reactant gas to be more fuel lean, whereas increasing the concentration of the reducing agent has the opposite affect. As the stoichiometric ratio increases, the NO_x reduction efficiency of noble metal catalysts decreases [68].

Ba promoted LNR over a Pt-only catalyst. This result is most obvious in Fig. 5, where the nitrous oxide concentration is shown as a function of inlet moles of NO_x. Here it can be seen that under steady state fuel lean conditions (i.e. >200 μmol inlet NO_x), the 1Pt/15Ba/5Fe catalyst has an N_2O concentration about 800 ppm higher than the 1Pt catalyst. The LNR results for the same two catalysts (not shown), showed that the 1Pt/15Ba/5Fe NO_x concentration was 5400 ppm, while the 1Pt NO_x concentration was 7700 ppm. The effect of Ba as a promoter for LNR was only evident when C_2H_4 was used as the reducing agent. However, even when C_2H_4 was the reductant, there was not always a significant difference in LNR for a Pt catalyst and Ba promoted Pt catalyst. It appears that the LNR promoter effect of Ba was strongly dependent on the reaction conditions.

3.1.4. Discussion

An alternative to considering the effect of reaction conditions on the catalytic performance is to consider the effect of the catalyst composition on the performance. This can be accomplished by comparing how the overall average for SNS, NOP, and LNR changes as a function of the catalytic composition. Because of the limited data set for this comparison, interactions between the metals were not considered in this analysis, and the confidence level was decreased to 90%. From this analysis, it was determined that each metal was significant for SNS, NOP, and/or LNR and therefore warranted further study. These results lead into the response surface study described in Section 4, where the effect of the three metals on the catalytic performance is examined more closely.

3.2. Sulfur poisoning

After completing the catalytic tests without sulfur, reaction condition 12 was chosen for the poisoning study, in which 300 ppm SO_2 was added by replacing a portion of the carrier gas with SO_2 such that the overall flowrate and remaining concentrations were held constant.

The poisoning study was preceded by heating the catalysts to 823 K in carrier gas and adding 10% v/v H_2 in He for 30 min. The catalysts were then cooled to 648 K in He and tested for six successive cycles of 14 min fuel lean and 6 min of fuel rich under reaction condition 12, without adding SO_2. The SO_2 was then added during both the fuel lean and fuel rich phases, and the catalysts were cycled in the same manner as described previously. After completing eight poisoning cycles, the inlet gases were switched to carrier gas and allowed to cool overnight in a continuous flow of carrier gas. On the second day, the catalysts were heated to 648 K, and six lean/rich cycles were completed without SO_2.

The SNS results are shown in Fig. 7. Before the SO_2 is added, the SNS is around 40 μmol of NO_x for the 1Pt/15Ba/5Fe catalyst. This was lower than the results shown in Fig. 3 of ~60 μmol NO_x for the Group 2 testing. All catalysts experienced a similar decrease in SNS between the Group 2 testing and the sulfur poisoning studies. This decrease could be due to changes that occurred to the catalysts while in ambient air between Group 2 testing and the poisoning studies, as indicated by [69]. Once SO_2 was added to the reaction gas stream, the catalysts immediately began to deactivate. By the thirteenth cycle, all catalysts were completely poisoned. Removing the SO_2 from the feed gas did not return the SNS capacity, demonstrating that the poisoning was permanent [25].

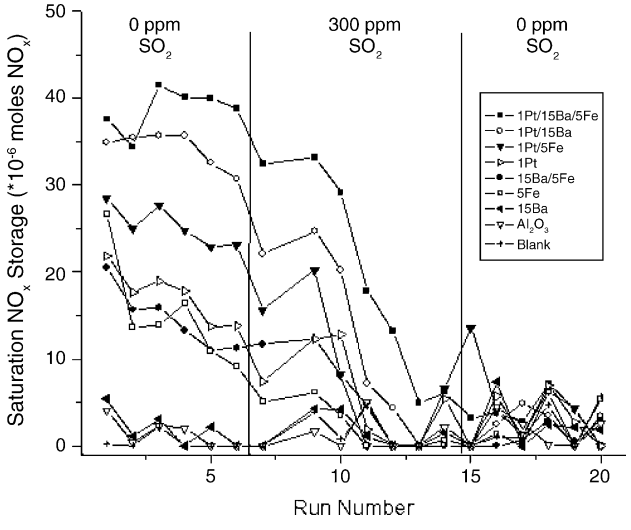

Fig. 7. The saturation NO_x storage is shown for all eight unique catalytic compositions in the screening design. Immediate degradation of the catalytic performance was observed upon the addition of SO_2 to the feed gas.

Iron was included as a catalytic composition parameter in this study because of a previous study indicating that the addition of Fe to a Pt/Ba NSR catalyst may improve resistance to sulfur poisoning [57]. As seen in Fig. 7, our results indicated at best a minimal effect from the addition of Fe. Upon the addition of SO_2 to the feed, the SNS of all catalysts decreased rapidly towards zero. It should be noted that SO_2 was only added during the fuel lean storage phase in [57] and not during both the fuel lean and fuel rich phases, as in the studies presented here. It has also been reported that NSR catalysts respond differently to SO_2 added under fuel lean or fuel rich conditions [25,26,31]. These previous reports have shown that the SO_2 deactivation mechanism under fuel lean conditions affected the NO_x storage component, while under fuel rich conditions the noble metal was deactivated. In [57], it was stated that the Fe improved the resistance to sulfur poisoning by decreasing the bond strength between Ba and SO_2. Our results, however, indicated that the Fe did not significantly affect the poisoning of the Pt, and therefore the overall SNS resistance to SO_2 was not significantly improved by the addition of Fe.

4. Response surface design

4.1. Experimental conditions

The screening study showed that Pt, Ba, and Fe all have an effect on the catalytic performance, and a nested response surface study was completed using a face centered central composite design for the catalyst compositions and a half fraction central composite design for the reaction conditions.

Ten additional catalysts for the response surface study were synthesized with additional weight loadings midway between the low and high weight loadings. Six catalysts were synthesized at the face centers of the three-dimensional parameter box (see Fig. 2), and are shown with a cross pattern. The remaining four catalyst were synthesized as center point catalysts, shown in gray in Fig. 2, to check for reproducibility in the catalyst synthesis procedure. Thus, 15 unique catalysts, plus three repeats, were used for this study. Since the reactor can only accommodate 16 catalysts, the experiments were completed in two stages. In Stage 1, the 15 unique compositions were loaded into the reactors, with one reactor left as a reference and referred to as the blank. In Stage 2, the center four catalysts were placed into three reactors each. The remaining four reactors were reserved as blanks. The data were analyzed to check for reproducibility in three different areas: reproducibility in the measured performance for the same catalyst in different reactors, reproducibility in the performance of catalysts with the same nominal loading, and reproducibility in the procedure used to calculate the SNS by using the four different reference reactors.

Only a subset of the response surface data is shown here. These data were collected in Stage 1 of the response surface study by measuring the catalytic performance for an inlet lean concentration of 2000 ppm v/v NO, 8% v/v O_2, 1% v/v CO at a temperature of 598 K and a space velocity of 42,500 mL/h/g catalyst. The data were collected during three subsequent cycles to provide an estimate of the reproducibility. The complete response surface dataset for the remaining reaction conditions and analysis will be reported in a forthcoming publication [70].

4.2. Results and discussion

Since the results for only one reaction condition are shown here, the effect of the reaction conditions on SNS, NOP, and LNR will not be discussed. However, since 15 unique catalytic compositions were tested, a more detailed analysis of the effect of the metals on the performance of the catalysts is shown. The results of this analysis for SNS and NOP are:

$$\mathrm{SNS} = 121(\pm 21)\mathrm{Pt} - 96(\pm 19)\mathrm{Pt}^2 + 2.7(\pm 1.4)\mathrm{Ba} - 0.15(\pm 0.09)\mathrm{Ba}^2 \quad (6)$$

$$\mathrm{NOP} = 2.6(\pm 1.6) + 26.6(\pm 5.0)\mathrm{Pt} - 22.2(\pm 4.5)\mathrm{Pt}^2 + 0.7(\pm 0.3)\mathrm{Ba} - 0.05(\pm 0.02)\mathrm{Ba}^2 + 0.07 \times (\pm 0.03)\mathrm{BaFe} \quad (7)$$

where SNS and NOP are given in micromoles NO_x and N_2O, respectively, and Pt, Ba and Fe are in weight percent. The 95% confidence intervals for the predicted SNS and NOP are ± 13.4 μmol NO_x and ± 3.1 μmol N_2O. Only the terms significant to 95% confidence, and their associated confidence intervals, are shown in Eqs. (6) and (7). For this reaction condition, there was minimal LNR and results are

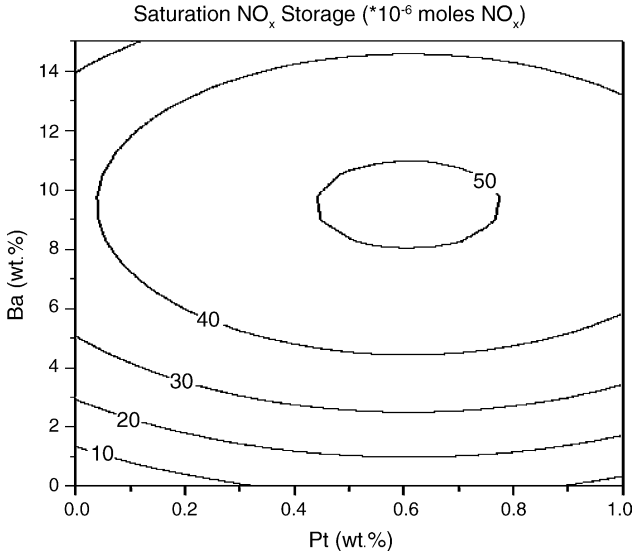

Fig. 8. The model prediction showing the saturation NO_x storage as a function of Pt and Ba weight loading. The maximum saturation NO_x storage is predicted at 0.63 wt.% Pt and 9.1 wt.% Ba.

Table 4
Comparison between the empirical models and experimental results

Catalyst name	SNS ($\times 10^{-6}$ mol NO_x)			NOP ($\times 10^{-6}$ mol N_2O)		
	Experimental mean	Standard deviation	Model prediction	Experimental mean	Standard deviation	Model prediction
0.6Pt/9.1Ba	33	4	51 ± 13	14	0.3	13 ± 3
0.65Pt/15Ba	42	19	46 ± 13	14	0.3	10 ± 3
0.5Pt/7.5Ba/2.5Fe	56	6	49 ± 13	21	0.3	14 ± 3

not shown for the effect of the catalytic composition on LNR.

The effect of the different metals is easier to see when the results are plotted as shown in Fig. 8, where the SNS is plotted as a function of Pt and Ba weight loading. Here it is seen that the predicted maximum in SNS occurs at a catalytic composition of 0.63% w/w Pt and 9.1% w/w Ba. This composition, however, is also very close to the maximum in predicted NOP and therefore it is not possible to achieve a maximum in SNS and a minimum in NOP for this condition. By relaxing the condition of achieving the maximum in SNS, one could make a catalyst with 0.65% w/w Pt and 15% w/w Ba that would have a predicted SNS 10% lower than the first catalyst, but the NOP would decrease by 24%. Both of these samples were prepared and tested, along with a 0.5Pt/15Ba/2.5Fe catalyst, in three successive cycles for SNS and NOP under the same conditions as previously mentioned. The experimental results along with the model predictions are listed in Table 4. The SNS for both the 0.65Pt/15Ba and 0.5Pt/7.5Ba/2.5Fe catalysts were within the range predicted by Eq. (6). The 0.6Pt/9.1Ba catalyst, however, stored less NO_x than predicted by the model. Since the weight loadings of these catalysts have not been confirmed, the actual weight loadings are unknown. The difference between the predicted NO_x storage and actual NO_x storage for the 0.6Pt/9.1Ba catalyst could be accounted for by this uncertainty. For the NOP, the model significantly underpredicted the nitrous oxide production for the 0.5Pt/7.5Ba/2.5Fe catalyst and slightly underpredicted the NOP production for the 0.65Pt/15Ba catalyst. These results indicate that the model at this point is to some extent incomplete and more refinement is necessary. More data are needed to accurately predict the SNS and NOP as a function of the catalytic composition.

The empirical model estimated in Eqs. (6) and (7) will change as the reaction conditions change. The final result will be a model that predicts the SNS, NOP, and LNR as a function of both the reaction conditions and the metal weight loadings. Once the response surface study is complete, a complete optimization procedure will be possible based on desired reaction conditions and performance.

5. Conclusions

In this study we have shown that the NO, O_2, reductant concentration, reductant type, space velocity, and temperature all have an effect on the performance of NSR catalysts. Further, the linear effects of these parameters have been estimated. It has also been shown that many parameters interact with each other, thus complicating the analysis of the data.

In addition to the reaction conditions, the effect of Pt, Ba, and Fe on NSR catalytic performance has been explored. It was concluded that all three metals affected the performance of NSR catalysts. SNS and NOP could be estimated for a given reaction condition as a function of Pt, Ba, and Fe weight loading. Additional work is underway to develop a more robust model to predict SNS, NOP, and LNR as a function of both reaction conditions and catalyst composition.

In general, because of the large quantity of data and the large array of experimental parameters that can be studied with HTE, it becomes increasingly imperative that statistical methods be employed to extract the information contained within the data. We have shown that HTE, in combination with DOE, can significantly increase the information content and subsequently the understanding obtained from high-throughput experimental data. It has also been shown that, by guiding HTE experiments using DOE, experimental resources can be used more efficiently to obtain the data required for model building.

Acknowledgements

The authors thank the National Science Foundation (Grant # 0343758-CTS) and Chemical Sciences, Geosciences and Biosciences Division, Office of Basic Energy Sciences, Office of Science, U.S. Department of Energy (Grant # DE-FG02-03ER15468) for funding this research work.

References

[1] R. Burch, J.P. Breen, F.C. Meunier, Appl. Catal. B 39 (2002) 283.
[2] V.I. Parvulescu, P. Grange, B. Delmon, Catal. Today 46 (1998) 233.
[3] J. Kaspar, P. Fornasiero, N. Hickey, Catal. Today 77 (2003) 419.
[4] S. Matsumoto, Catal. Today 29 (1996) 43.
[5] S.I. Matsumoto, Y. Ikeda, H. Suzuki, M. Ogai, N. Miyoshi, Appl. Catal. B 25 (2000) 115.
[6] H. Hirata, I. Hachisuka, Y. Ikeda, S. Tsuji, S.I. Matsumoto, Top. Catal. 16/17 (2001) 145.

[7] N. Takahashi, H. Shinjoh, T. Iijima, T. Suzuki, K. Yamazaki, K. Yokota, H. Suzuki, N. Miyoshi, S. Matsumoto, T. Tanizawa, T. Tanaka, S. Tateishi, K. Kasahara, Catal. Today 27 (1996) 63.
[8] W. Bögner, M. Krämer, B. Krutzsch, S. Pischinger, D. Voigtänder, G. Wenninger, F. Wirbeleit, M.S. Brogan, R.J. Brisley, D.E. Webster, Appl. Catal. B 7 (1995) 153.
[9] L. Olsson, H. Persson, E. Fridell, M. Skoglundh, B. Andersson, J. Phys. Chem. B 105 (2001) 6895.
[10] B. Westerberg, E. Fridell, J. Mol. Catal. A: Chem. 165 (2001) 249.
[11] P.H. Han, Y.K. Lee, S.M. Han, H.K. Rhee, Top. Catal. 16/17 (2001) 165.
[12] F. Prinetto, G. Ghiotti, I. Nova, L. Lietti, E. Tronconi, P. Forzatti, J. Phys. Chem. B 105 (2001) 12732.
[13] L. Lietti, P. Forzatti, I. Nova, E. Tronconi, J. Catal. 204 (2001) 175.
[14] C. Hess, J.H. Lunsford, J. Phys. Chem. B 106 (2002) 6358.
[15] C. Sedlmair, K. Seshan, A. Jentys, J.A. Lercher, J. Catal. 214 (2003) 308.
[16] D. James, E. Fourre, M. Ishii, M. Bowker, Appl. Catal. B 45 (2003) 147.
[17] F. Rodrigues, L. Juste, C. Potvin, J.F. Tempere, G. Blanchard, G. Djega-Mariadassou, Catal. Lett. 72 (2001) 59.
[18] H. Mahzoul, J.F. Brilhac, P. Gilot, Appl. Catal. B 20 (1999) 47.
[19] H. Mahzoul, P. Gilot, J.F. Brilhac, B.R. Stanmore, Top. Catal. 16 (2001) 293.
[20] A. Amberntsson, H. Persson, P. Engstrom, B. Kasemo, Appl. Catal. B 31 (2001) 27.
[21] J. Despres, M. Koebel, O. Krocher, M. Elsener, A. Wokaun, Appl. Catal. B 43 (2003) 389.
[22] G. Centi, G.E. Arena, S. Perathoner, J. Catal. 216 (2003) 443.
[23] S. Hodjati, K. Vaezzadeh, C. Petit, V. Pitchon, A. Kiennemann, Appl. Catal. B 26 (2000) 5.
[24] K. Vaezzadeh, C. Petit, V. Pitchon, A. Kiennemann, Catal. Commun. 3 (2002) 179.
[25] A. Amberntsson, M. Skoglundh, S. Ljungstrom, E. Fridell, J. Catal. 217 (2003) 253.
[26] E. Fridell, H. Persson, L. Olsson, B. Westerberg, A. Amberntsson, M. Skoglundh, Top. Catal. 16 (2001) 133.
[27] P. Engstrom, A. Amberntsson, M. Skoglundh, E. Fridell, G. Smedler, Appl. Catal. B 22 (1999) 241.
[28] A. Amberntsson, M. Skoglundh, M. Jonsson, E. Fridell, Catal. Today 73 (2002) 279.
[29] A. Amberntsson, B. Westerberg, P. Engstrom, E. Fridell, M. Skoglundh, Stud. Surf. Sci. Catal. 126 (1999) 317.
[30] H.Y. Huang, R.Q. Long, R.T. Yang, Appl. Catal. B 33 (2001) 127.
[31] C. Sedlmair, K. Seshan, A. Jentys, J.A. Lercher, Catal. Today 75 (2002) 413.
[32] C. Sedlmair, K. Seshan, A. Jentys, J.A. Lercher, Res. Chem. Intermed. 29 (2003) 257.
[33] P.T. Fanson, M.R. Horton, W.N. Delgass, J. Lauterbach, Appl. Catal. B 46 (2003) 393.
[34] J.P. Breen, M. Marella, C. Pistarino, J.R.H. Ross, Catal. Lett. 80 (2002) 123.
[35] S. Senkan, Angew. Chem. Int. Ed. 40 (2001) 312.
[36] R.A. Potyrailo, E.J. Amis (Eds.), High Throughput Analysis: A Tool of Combinatorial Materials Science, Plenum Pub. Corp., 2004.
[37] K. Krantz, S. Ozturk, S. Senkan, Catal. Today 62 (2000) 281.
[38] S. Ozturk, S. Senkan, Appl. Catal. B 38 (2002) 243.
[39] A. Richter, M. Langpape, S. Kolf, G. Grubert, R. Eckelt, J. Radnik, A. Schneider, M.M. Pohl, R. Fricke, Appl. Catal. B 36 (2002) 261.
[40] O.M. Busch, C. Hoffmann, T.R.F. Johann, H.W. Schmidt, W. Strehlau, F. Schuth, J. Am. Chem. Soc. 124 (2002) 13527.
[41] J. Lawson, J. Erjavec, Modern Statistics for Engineering and Quality Improvement, Brooks/Cole-Thomson Learning, Pacific Grove, CA, 2000.
[42] M. Tagliabue, L.C. Carluccio, D. Ghisletti, C. Perego, Catal. Today 81 (2003) 405.
[43] D.S. Bem, R.D. Gillespie, E.J. Erlandson, L.A. Harmon, S.G. Schlosser, A.J. Vayda, in: J.N. Cawse (Ed.), Experimental Design for High Throughput Materials Development, Wiley, Hoboken, NJ, 2003, p. 89.
[44] J.L. Spivack, J.N. Cawse, D.W. Whisenhunt Jr., B.F. Johnson, K.V. Shalyaev, J. Male, E.J. Pressman, J.Y. Ofori, G.L. Soloveichik, Appl. Catal. A 254 (2003) 5.
[45] J. Urschey, A. Kuhnle, W.F. Maier, Appl. Catal. A 252 (2003) 91.
[46] L. Harmon, J. Mater. Sci. 38 (2003) 4479.
[47] I.E. Maxwell, P. van den Brink, R.S. Downing, A.H. Sijpkes, S. Gomez, T. Maschmeyer, Top. Catal. 24 (2003) 125.
[48] C.M. Snively, S. Katzenberger, G. Oskarsdottir, J. Lauterbach, Opt. Lett. 24 (1999) 1841.
[49] C.M. Snively, G. Oskarsdottir, J. Lauterbach, J. Comb. Chem. 2 (2000) 243.
[50] C.M. Snively, G. Oskarsdottir, J. Lauterbach, Angew. Chem. Int. Ed. 40 (2001) 3028.
[51] C.M. Snively, G. Oskarsdottir, J. Lauterbach, Catal. Today 67 (2001) 357.
[52] C.M. Snively, J. Lauterbach, Spectroscopy 17 (2002) 26.
[53] R.J. Hendershot, S.S. Lasko, M.F. Fellmann, G. Oskarsdottir, W.N. Delgass, C.M. Snively, J. Lauterbach, Appl. Catal. A 254 (2003) 107.
[54] R.J. Hendershot, P.T. Fanson, C.M. Snively, J. Lauterbach, Angew. Chem. Int. Ed. 42 (2003) 1152.
[55] G.E.P. Box, W.G. Hunter, J.S. Hunter, Statistics for Experimenters: An Introduction to Design, Data Analysis and Model Building, Wiley, New York, 1978.
[56] C.R. Hicks, K.V. Turner, Fundamental Concepts in the Design of Experiments, 5th ed. Oxford University Press, New York, 1999.
[57] K. Yamazaki, T. Suzuki, N. Takahashi, K. Yokota, M. Suguira, Appl. Catal. B 30 (2001) 459.
[58] E. Fridell, M. Skoglundh, B. Westerberg, S. Johansson, G. Smedler, J. Catal. 183 (1999) 196.
[59] S. Balcon, C. Potvin, L. Salin, J.F. Tempere, G. Djega-Mariadassou, Catal. Lett. 60 (1999) 39.
[60] F. Acke, M. Skoglundh, Appl. Catal. B 20 (1999) 133.
[61] R. Burch, J.A. Sullivan, T.C. Watling, Catal. Today 42 (1998) 13.
[62] S. Poulston, R.R. Rajaram, Catal. Today 81 (2003) 603.
[63] N.W. Cant, M.J. Patterson, Catal. Lett. 85 (2003) 153.
[64] M.H. Thiemens, W.C. Trogler, Science 251 (1991) 932.
[65] C. Rottlander, R. Andorf, C. Plog, B. Krutzsch, M. Baerns, J. Catal. 169 (1997) 400.
[66] R. Burch, S.T. Daniells, P. Hu, J. Chem. Phys. 117 (2002) 2902.
[67] H. Shinjoh, T. Tanabe, H. Sobukawa, M. Sugiura, Top. Catal. 16 (2001) 95.
[68] H.S. Gandhi, G.W. Graham, R.W. McCabe, J. Catal. 216 (2003) 433.
[69] G.W. Graham, H.W. Jen, J.R. Theis, R.W. McCabe, Catal. Lett. 93 (2004) 3.
[70] R.J. Hendershot, W.B. Rogers, C.M. Snively, B.A. Ogunnaike, J. Lauterbach, in preparation.